Indian Journal of Pure & Applied Physics
Vol. 62, March 2024, pp. 189-195
DOI: 10.56042/ijpap.v62i3.7003

Ab-initio Study of Vibrational Properties of the Most Stable ZnTe Nanoclusters

Dheeraj Kumar Pandey[a*], Anilesh[b] & P S Yadav[c]

[a]Department of Physics, R. B. College (A Constituent College of Lalit Narayan Mithila University, Darbhanga), Dalsingsarai, Samastipur, Bihar 848 114, India

[b]Department of Physics, R. N. A. R. College (A Constituent College of Lalit Narayan Mithila University, Darbhanga), Samastipur, Bihar 848 101, India

[c]Department of Physics, University of Allahabad, Prayagraj, Uttar Pradesh 211 002, India

Received 29 November 2023; accepted 15 January 2024

An ab-initio investigation has been conducted for exploring the vibrational properties of very small size Zn_xTe_y (x + y = 2 to 5 atoms) nanoclusters, which are obtained by density functional theory method (B3LYP-DFT/LANL2DZ). We have predicted here the vibrational frequencies, Infrared intensities (IR), Relative Infrared intensities and Raman scattering activities of the most stable Zn_xTe_y (x + y = 2 to 5 atoms) nanoclusters. The structure having minimum energy in comparison to other structures having same values of "x" and "y" is considered as most stable. The zero point energy correction is also considered. $ZnTe_4$ nanoclusters do not show any stable structure as all their configurations have at least one or more imaginary vibrational frequencies leading to their instability. The vibrational frequencies having higher values of each most stable nanocluster corresponds to the asymmetrical and symmetrical stretching vibrations whereas the frequencies having lower values corresponds to rocking, breathing, wagging and the out of plane vibrations of Zn and Te atoms of their corresponding nanocluster.

Keywords: Nanoclusters, Vibrational properties, Raman Activity, IR Intensity, DFT study

1 Introduction

More than three decades, nanomaterials of semiconducting behavior have drawn our strong concentration due to their wide range of applications because of having various new fascinating substantial and chemical properties[1–4]. Among semiconductor materials II–VI semiconductors are predominantly fascinating and have been focused in a lot of experimental and theoretical investigations in latest years[5-9]. The II–VI semiconductor materials are a special class of prevalent nanomaterials. Generally, a nanocluster is defined as an intermediate stage amid molecule and bulk[10,11]. The ratio of surface area and volume in nanoclusters is relatively high in contrast to the subsequent bulk stage[12,13]. The studies of nanoclusters have fascinated huge attention of researchers as their optical and electronic properties confirm noticeably variation from their consequent bulkiness properties because of quantum confinement effect.

In the midst of II–VI compound semiconductors, Zinc Telluride (ZnTe) is a direct band gap semiconducting material having band gap of 2.26 eV (~548 nm) at room temperature. It has several probable applications in solar cells and blue green light emitting diodes (LEDs)[14,15]. In addition to ZnTe material is that it also posses' p-type conductivity owing to the occurrence of Zn vacancies[16]. However, research on ZnTe nanomaterials acknowledged very fewer concentrations in comparison to its other contemporaries, which is possibly because of being short of suitable precursor[17,18] and not as much of stability of ZnTe nanomaterials in the air other than chalcogenides[19]. Presently, the ZnTe nanomaterial is mostly produced by evaporating ZnTe powder with using only gold as catalyst at very high temperature of about 900 °C[20,21]. Further ZnTe nanomaterials like nanorods and nanowires are also produced by wet chemical method and largely implicated the explode nucleation and further aggregation of the monomers created by precursors[22,23]. A large number of experimental procedures have been also engaged by many researchers to synthesize the Zinc Telluride nanomaterials[24–28]. Chávez *et al.*[24] have synthesized ZnTe nanoparticle by mechanochemical synthesis procedure, while Dwivedi *et al.*[28] attempted to synthesize ZnTe nanoparticles by chemical synthesis method.

*Corresponding author:
(E-mail: dheerajgkp85@gmail.com; pdhiraj2000@gmail.com)

Although the real-world application of semiconducting nonmaterial requires extensive experimental research, theoretical approaches are of fundamental importance as they allow both to realize the elementary physics and to optimize devices made from nanostructure materials. There have been numerous theoretical investigations of the structural stabilities, electronic (HOMO–LUMO gaps) and optical properties of several $(ZnTe)_n$ type nanoclusters[29,30]. Earlier, we have reported an exhaustive ab-initio investigations of structural and electronic properties of ZnTe upto five atom nanoclusters[31] but the other substantial properties like vibrational properties for the mainly stable Zn_xTe_y (x + y = 2 to 5 atoms) nanoclusers have not been explored so far up to the knowledge of us. Now in this paper, we have extended our ab-initio investigation for vibrational properties of the most stable Zn_xTe_y nanoclusters. Here, we report the results of normal mode of vibrations, Infrared Intensities (IR) Relative Infrared Intensities and Raman Activity of small size most stable Zn_xTe_y (x + y = 2 to 5) nanoclusters. The present study also draws the attention of experimental researchers to synthesize these nanoclusters for their possible applications in fabrication of nanodevices. Section 2 contains the method employed in the investigations. In Section 3, we have described the calculation and results. The last Section 4 contains the conclusions.

2 Materials and Method

The structural optimizations of the ZnTe nanoclusters are obtained by employing the B3LYP-DFT/LANL2DZ edition in the Gaussian-03 code[32] which uses the hierarchy of procedures equivalent to unlike approximation methods. By analytical differentiation of gradient, the harmonic vibrational frequencies of nanoclusters of different structures are calculated. In the Hartree-Fock theory, the exact exchange for a single determinant is replaced in the Density Functional Theory (DFT) by another common expression, the exchange-correlation functional which contains terms accountable for both, the electron correlation and the exchange energy.

In this investigation, we consider the correlation function of Lee, Yang and Parr (LYP) and the Becke exchange functional that includes assistance for both the nonlocal and local. Also, we have used Becke's three parameter hybrid functional. Here, Becke functional uses the Slater exchange besides the corrections involving the gradient of the density (Becke). We also use a basis set LANL2DZ which is essential for the explanation of the ground state of every atom. The interior electrons are replaced by efficient core potential in LANL2DZ basis sets. The pseudo potential approximation is to substitute the combined effects of motion of bound electrons of an atom and the efficient potential of the nucleus is mentioned as pseudo potential in which the Schrödinger equation posses a customized potential term. Since, Zinc and Tellurium has the atomic number of 30 and 52 respectively, LANL2DZ basis set will provide a better results with pseudo potential approximation. This is the reason why B3LYP/ LANL2DZ basis set is selected to completely optimize the Zn_xTe_y nanoclusters.

3 Calculation and Results

In order to obtaining the most stable ZnTe nanoclusters, various types of all probable structures including the linear chains, planer, rings and three-dimensional ones for each configuration have been considered[31]. Each structure is obtained to its least amount of energy by comforting the atomic coordinates. The relaxation in the system energy up to 10^{-7} meV and the minimum forces of 10^{-3} eV/Å on each atom were achieved. The structure for each configuration having minimum energy in comparison to other structures possessing same value of "x" and "y" is considered as most stable. The zero point energy correction is also considered for the purpose of obtaining stability of these nanoclusters. In the stability of these nanostructures the harmonic vibrational frequencies are also studied. The imaginary vibrational frequency for a structure points to its instability.

3.1 Vibrational properties

The normal modes of vibration of each individual nanocluster are obtained by the calculation of the second derivatives of the total energy of the corresponding nanocluster as a system with respect to their atomic displacements. Further this obtained dynamical matrix is then diagonalized. The above calculation provides substantial quantities for each and every the most stable ZnTe nanoclusters up to five atoms, which are presented in Table 1. In the table, the brackets subsequent the frequencies restrain the multiplicity of the vibrational mode. All potential modes of vibrations of each and every most stable nanocluster of Fig. 1 are shown in Figs. 2–8. In these figures, the arrow heads indicate the trend and degree of the displacements of atoms for the duration of the

Table 1 — The calculated vibrational frequencies (cm^{-1}), Infrared intensities (IR Int. in km mol^{-1}), relative IR intensities (Rel. IR Int.) and Raman scattering activities (Raman activity in A^4/ amu) of Zn_xTe_y (x + y = 2 to 5). Brackets following the frequencies contain the multiplicity of the mode.

Configuration	Properties	Values
Linear ZnTe (1a)	Frequency	122
	IR Int.	0.98
	Rel. IR Int.	1.0
	Raman activity	18.10
Linear TeZnTe (1b)	Frequencies	43(2), 123, 261
	IR Int.	3.01, 0.00, 29.22
	Rel. IR Int.	0.10, 0.00, 1.00
	Raman activity	0.00, 50.39, 0.00
Linear ZnTeZn (1c)	Frequencies	34 (2), 137, 140
	IR Int.	8.58, 12.66, 0.00
	Rel. IR Int.	0.68, 1.00, 0.00
	Raman activity	0.00, 0.00, 10.42
Rhombus $ZnTe_3$ (1d)	Frequencies	31, 51, 75, 97, 178, 225
	IR Int.	1.75, 2.00, 1.16, 0.06, 2.42, 6.56
	Rel. IR Int.	0.27, 0.30, 0.18, 0.00, 0.37, 1.00
	Raman activity	2.35, 11.13, 3.86, 8.25, 28.35, 1.15
Rhombus Zn_2Te_2 (1e)	Frequencies	66, 118, 131, 166, 191, 231
	IR Int.	4.37, 0.00, 7.98, 0.00, 0.00, 25.00
	Rel. IR Int.	0.17, 0.00, 0.32, 0.00, 0.00, 1.00
	Raman activity	0.00, 14.03, 0.00, 2.49, 34.16, 0.00
Linear ZnZnTeZn (1f)	Frequencies	11(2), 36(2), 61, 110, 190
	IR Int.	0.85, 5.03, 6.58, 15.64, 1.18
	Rel. IR Int.	0.05, 0.30, 0.42, 1.00, 0.08
	Raman activity	3.85, 2.21, 2.03, 0.60, 67.17
Pentagonal 2 Zn_2Te_3 (1g)	Frequencies	21, 60, 69, 103, 124, 145, 149, 227, 259
	IR Int.	0.00, 4.22, 1.66, 0.18, 5.20, 0.63, 0.18, 1.23, 28.96
	Rel. IR Int.	0.00, 0.15, 0.06, 0.00, 0.18, 0.02, 0.00, 0.04, 1.00
	Raman activity	1.05, 0.13, 3.96, 9.97, 1.93, 4.65, 35.26, 0.03, 1.36
Pentagonal Zn_3Te_2 (1h)	Frequencies	57, 57, 83, 88, 120, 149, 154, 220, 154, 220, 250
	IR Int.	2.42, 0.00, 0.84, 0.33, 5.25, 1.03, 4.25, 9.01, 15.92
	Rel. IR Int.	0.15, 0.00, 0.05, 0.02, 0.33, 0.06, 0.27, 0.59, 1.00
	Raman activity	0.06, 0.76, 9.80, 5.69, 1.71, 54.13, 0.68, 1.72, 1.73
Planar Zn_4Te (1i)	Frequencies	15, 18, 42, 55, 64, 75, 112, 127, 149
	IR Int.	0.09, 1.14, 4.42, 1.67, 6.57, 3.08, 3.26, 0.16, 2.67
	Rel. IR Int.	0.01, 0.17, 0.67, 0.25, 1.00, 0.47, 0.50, 0.02, 0.41
	Raman activity	5.71, 2.10, 0.06, 3.02, 10.66, 63.56, 49.78, 5.39, 22.84

different modes of vibration, while very small displacement (below 0.10 Å) is ignored. We have also obtained and presented the infrared (IR) intensities, relative infrared (IR) intensities and Raman scattering activities (Raman Activity) in the table. The above substantial properties have not been reported by any other workers. We discuss the above substantial properties of each nanocluster below:

ZnTe

For two atoms ZnTe nanocluster (Fig. 2(a)), we find the stretching mode frequency of 122 cm^{-1}, while Olego *et al*.[33] has reported the vibrational frequency as 209 cm^{-1}. This vibrational frequency of ZnTe nanocluster is both infrared and Raman-active.

Zn_xTe_y (x+y = 3)

$ZnTe_2$: For the linear TeZnTe structure (Fig. 1(b)), we find the four normal modes of vibrational frequencies. The asymmetric stretching vibration (Fig. 2(d)) of the Zn and Te atoms along the chain appears as the highest frequency of 261 cm^{-1} for the linear TeZnTe structure. The mid frequency of 123 cm^{-1} (Fig. 2(c)) arises due to the breathing vibrations of Te atoms. The lowest doublet vibrational frequency of 43 cm^{-1} (Fig. 2(b)) arises due to the bending vibration. The mid vibrational frequency is Raman active but not infrared active while the lowest and highest vibrational frequencies are infrared active but not Raman-active.

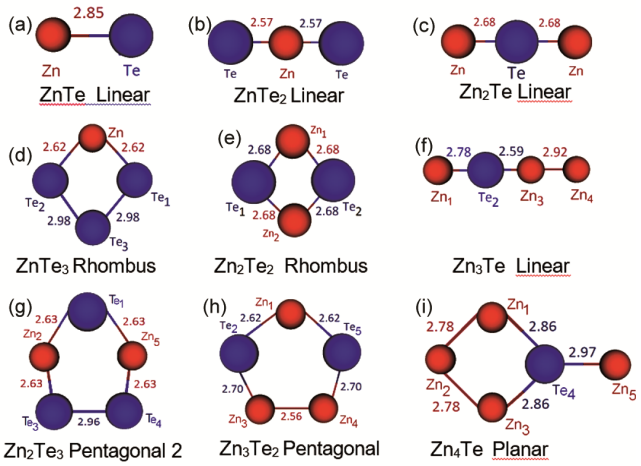

Fig. 1 — Most stable structures of ZnTe, $ZnTe_2$, Zn_2Te, $ZnTe_3$, Zn_2Te_2, Zn_3Te, Zn_2Te_3, Zn_3Te_2, and Zn_4Te nanocluster. (All the bond lengths are in A^0).

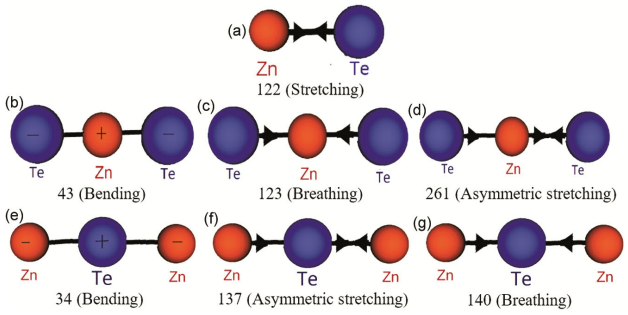

Fig. 2 — Normal modes of vibrations of most stable ZnTe Linear, $ZnTe_2$ Linear and Zn_2Te Linear nanoclusters. The numbers are the frequencies in cm^{-1}. The nature of vibration is given inside brackets.

Zn_2Te: The three normal modes of vibrations have been obtained for linear ZnTeZn structure (Fig. 1(c)). The maximum frequency of 140 cm^{-1} (Fig. 2(g)) arises due to the breathing vibrations of all the atoms. The asymmetric stretching vibration (Fig. 2(f)) of linear ZnTeZn structure has frequency of 137 cm^{-1}. The lowest frequency 34 cm^{-1} (Fig. 2(e)) arises due to the bending vibration of the linear ZnTeZn nanocluster. Except the highest frequency, all the vibrational frequencies are infrared active but only the highest vibrational frequency is Raman-active.

Zn_xTe_y (x+y = 4)

$ZnTe_3$: For the rhombus $ZnTe_3$ structure (Fig. 1(d)), we find six normal modes of vibrational frequencies. The wagging vibration (Fig. 3(a)) appears due to the lowest vibrational frequency of 31 cm^{-1} while the asymmetric vibration of Te – Te bonds (Fig. 3(f)) appears due to the highest frequency of 255 cm^{-1}. The out of plane vibration (Fig. 3(b)), asymmetric

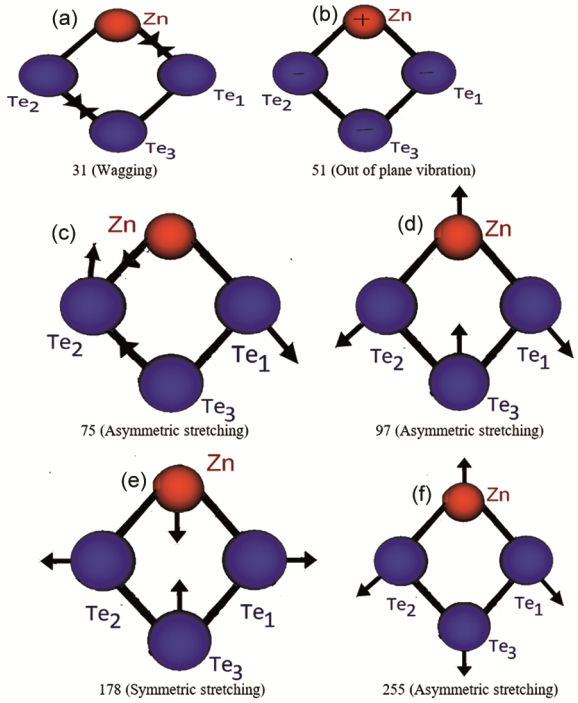

Fig. 3 — Normal modes of vibrations of most stable $ZnTe_3$ Rhombus nanocluster. The numbers are the frequencies in cm^{-1}. The nature of vibration is given inside brackets.

stretching (Fig. 3(c), 3(d)) and symmetric stretching (Fig. 3(e)) vibrations appears because of other mid frequencies 51, 75, 97 and 178 cm^{-1} of the rhombus $ZnTe_3$ structure. Both the highest and lowest vibrational frequencies are infrared and Raman-active.

Zn_2Te_2: There are also six normal modes of vibrational frequencies for the rhombus Zn_2Te_2 structure (Fig. 1(e)). The breathing vibrations (Fig. 4(f)) of Zn and Te atoms appears because of the highest vibrational frequency of 231 cm^{-1}, while the out of plane vibration (Fig. 4(a)) of Zn and Te atoms appears due to the lowest vibrational frequency of 66 cm^{-1}. Other mid vibrational frequencies arise due to symmetric stretching (Fig. 4(b), asymmetric stretching vibrations (Fig. 4(c&e)) and rocking vibration (Fig. 4(d)). Some vibrational frequencies are either Raman active or infrared active.

Zn_3Te: The linear ZnZnTeZn structure (Fig. 1(f)) has seven normal modes of vibrational frequency. The low lying one of the doublet frequency of 11 cm^{-1} arises from the out of plane vibration of Te and Zn atoms while the frequency 36 cm^{-1} originates from the symmetric stretching vibration (Fig 5(c)). The two mid vibrational frequencies (second frequency of doublet) 11 and 36 cm^{-1} arise due to out of plane

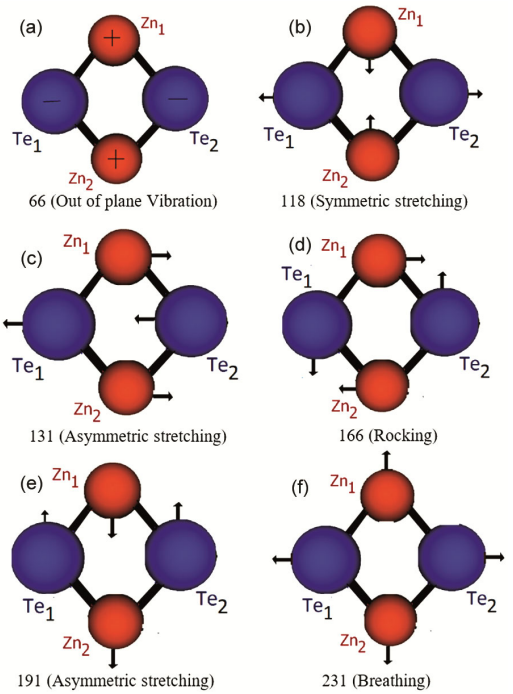

Fig. 4 — Normal modes of vibrations of most stable Zn_2Te_2 Rhombus nanocluster. The numbers are the frequencies in cm^{-1}. The nature of vibration is given inside brackets.

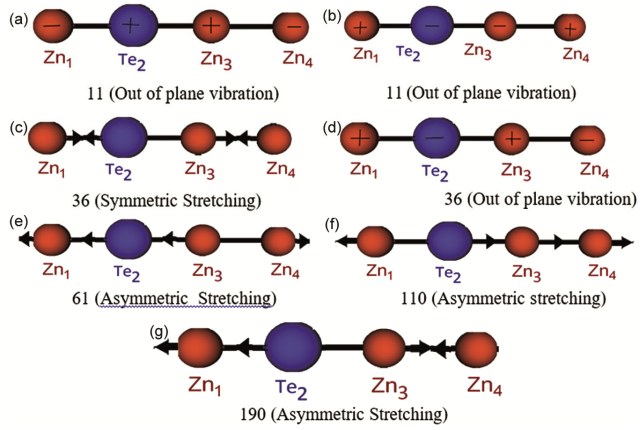

Fig. 5 — Normal modes of vibrations of most stable Zn_3Te Linear nanocluster. The numbers are the frequencies in cm^{-1}. The nature of vibration is given inside brackets.

vibration (Fig. 5(b&d)), while other higher frequencies 61, 110 and 190 cm^{-1} arise due to asymmetric stretching vibrations (Fig. 5(e,f&g), respectively. All the vibrational frequencies are both infrared and Raman active.

Zn_xTe_y (x+y = 5)

Each and every investigated structures of $ZnTe_4$ configuration possess at least one imaginary frequency and due to this they are considered as unstable structures.

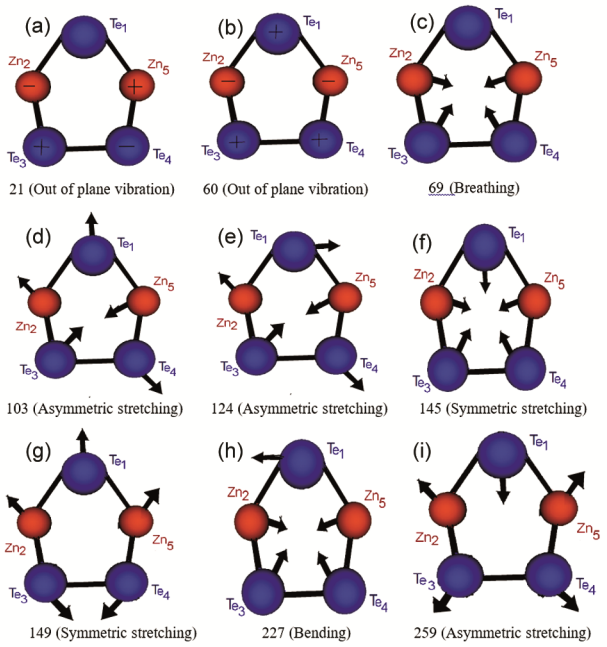

Fig. 6 — Normal modes of vibrations of most stable Zn_2Te_3 Pentagonal nanocluster. The numbers are the frequencies in cm^{-1}. The nature of vibration is given inside brackets.

Zn_2Te_3: The pentagonal Zn_2Te_3 structure (Fig. 1(g)) has nine normal modes of vibrational frequencies. The asymmetric stretching vibration (Fig. 6(i)) appears due to the highest vibrational frequency of 259 cm^{-1}. There are two out of plane vibrations (Fig. 6(a&b)) of Zn and Te atoms for pentagonal Zn_2Te_3 structure, which corresponds to the vibrational frequencies of 21 and 60 cm^{-1}. All the others vibrational frequencies arise due to asymmetric stretching, symmetric stretching, breathing and bending vibrations. Further, for pentagonal Zn_2Te_3 structure most of the vibrational frequencies are infrared active and Raman active.

Zn_3Te_2: The pentagonal Zn_3Te_2 structure (Fig. 1(h)), has also nine normal modes of vibrational frequencies. The asymmetric stretching vibration (Fig. 7(i)) appears because of the highest vibrational frequency of 250 cm^{-1}. The doublet frequency 57 cm^{-1} arises from the out of plane vibrations (Fig. 7(a&b)) of Zn and Te atoms. All others vibrational frequencies arise because of stretching, bending and breathing vibrations. For pentagonal Zn_3Te_2 structure, the most of vibrational frequencies are infrared active and Raman active.

Zn_4Te: For the Planar Zn_4Te (Fig. 1(i)) structure, we find nine normal modes of vibrational frequencies. The asymmetric stretching vibration of the Planar Zn_4Te structure appears due to the highest vibrational

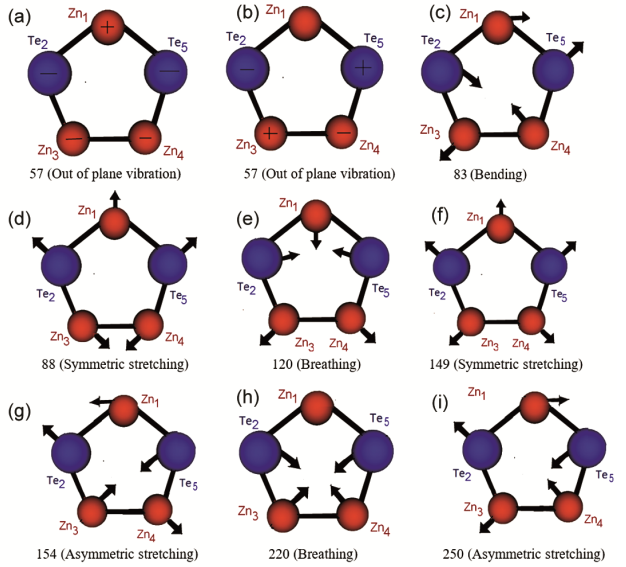

Fig. 7 — Normal modes of vibrations of most stable Zn_3Te_2 Pentagonal nanocluster. The numbers are the frequencies in cm^{-1}. The nature of vibration is given inside brackets.

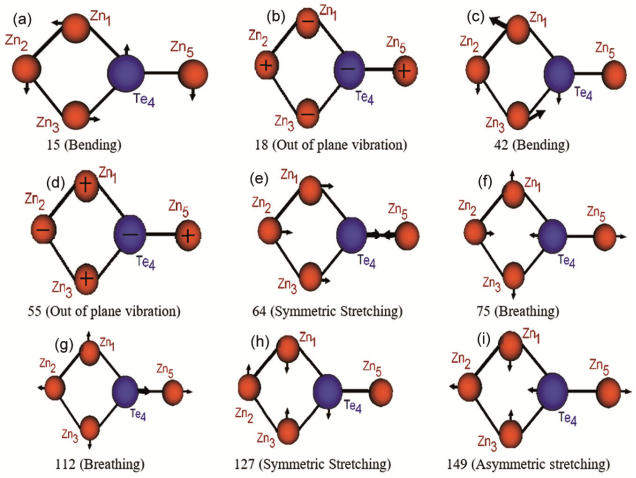

Fig. 8 — Normal modes of vibrations of most stable Zn_3Te_2 Planer nanocluster. The numbers are the frequencies in cm^{-1}. The nature of vibration is given inside brackets.

frequency of 149 cm^{-1}. The two mid vibrational frequencies of 18 and 55 cm^{-1} arises because of the out of plane vibrations of Zn and Te atoms (Fig. 8(b&d)). All the others rest vibrational frequencies of the Planar Zn_4Te structure arise due to stretching, breathing and bending vibrations. The most of the vibrational frequencies are infrared active and Raman active.

The above investigation of the different normal modes of vibrations of the various most stable structures revels that the asymmetrical and symmetrical stretching vibrations appears because of the high vibrational frequencies. In addition to this, the lower vibrational frequencies correspond to the rocking, breathing, wagging and the out of plane vibrations of Zn and Te atoms of their corresponding ZnTe nanocluster. The above discussion also reveals that each and every investigated nanocluster of $ZnTe_4$ configuration has no any stable structure because of all the possible ZnTe structures have at least one or more imaginary vibrational frequencies.

4 Conclusion

This present study explores the vibratonal properties of mainly the highest stable structures up to five atoms of ZnTe nanoclusters. We have predicted the vibrational frequencies, Infrared Intensities (IR), Relative Infrared Intensities and Raman scattering activities, which needed to be verified by experimental researches. For x + y = 5, we obtain that Zn_2Te_3, Zn_3Te_2 and Zn_4Te configurations are stable but on the other hand $ZnTe_4$ configuration has no any stable structure because of all the investigated structures of this configuration has at least one or more imaginary vibrational frequencies. The above study shows that the high vibrational frequencies arise from the asymmetrical and symmetrical stretching vibrations whereas the lower frequencies belong to breathing, rocking, wagging and the out of plane vibrations of Zn and Te atoms of their corresponding ZnTe nanocluster. This theoretically establishes nanoclusters will draw the attention of experimental researchers to synthesize these nanoclusters for their possible applications in fabrication of nanodevices according to their explored physical properties.

Acknowledgement

The authors are thankful to Lalit Narayan Mithila University, Darbhanga, Bihar, India for support. The present work has been performed at Condensed Matter Physics Research Laboratory (CMPRL), Department of Physics, University of Allahabad, Prayagraj, Uttar Pradesh, India.

References

1 Jr M B, Moronne M, Gin P, Weiss S & Alivisatos A P, *Science*, 281 (1998) 2013.
2 Biju V, Itoh T, Anas A, Sujith & Ishikawa M, *Anal Bioanal Chem*, 391(2008) 2469.
3 Bidoz S F, Jennings T, Klostranec J M, Fung W, Rhee A, Li D & Chan W C W, *Angew Chem Int Ed*, 47 (2008) 5577.
4 *Wang D S, He J & Rosenzweig N,* Nano Lett*, 4 (2004) 409.*
5 Goodrow A, Bel AT & Gordon M H, *J Chem Phys*, 129 (2008) 174109.

6 Wang C, Zhang H, Li M, Sun H & Yang B, *J Phys Chem C*, 111 (2007) 2465.
7 De T T, O'Brien P & Pickett N L, *Chem Mater*, 13 (2001) 3843.
8 Murray B, Kagan C R & Bawendi M G, *Ann Rev Mater Sci*, 30 (2000) 545.
9 Wang X Q, Clark S J & Abram R A, *Phys Rev B,* 70 (2004) 235328.
10 Bernstien E R, Atomic and molecular clusters Studies in Physical and Theoretical chemistry, Amsterdam: Elsevier, 68 (1990).
11 Jena P, Rao B K & Khanna S N, Physics and chemistry of small clusters (NATO ASI Series), Dordrecht: Kluwer, 158 (1990).
12 Himmel H J & Hebben N, *Chem Eur J*, 11 (2005) 4096.
13 Sheehan S M, Meloni G, Parsons B F, Wehres N & Neumark D M, *J Chem Phys*, 124 (2006) 064303.
14 Hou L, Zhang Q, Ling L, Li C X, Chen L & Chen S, *J Am Chem Soc*, 135 (2013) 10618.
15 Jang Y J, Jeong I, Lee J, Ko M J & Lee J S, *ACS Nano*, 10 (2016) 6980.
16 Crisp R W, Pach G F, Kurley J M, France R M, Reese M O, Nanayakkara S U, MacLeod B A, Talapin D V, Beard M C & Luther J M, *Nano Lett*, 17 (2017) 1020.
17 Zhang J, Sun K, Kumbhar A & Fang J Y, *J Phys Chem C,* 112 (2008) 5454.
18 Jiang F, Li Y, Ye M, Fan L, Ding Y & Li Y*, Chem Mater,* 22 (2010) 4632.
19 Reiss P, Carriere M, Lincheneau C, Vaure L & Tamang S, *Chem Rev*, 116 (2016) 10731.
20 Utama M I B, Mata M, Zhang Q, Magen C, Arbiol J & Xiong Q H, *Cryst Growth Des*, 13 (2013) 2590.
21 Wu D, Jiang Y, Zhang Y, Li J, Yu Y, Zhang Y, Zhu Z, Wang L, Wu C & Jee J, *Nanotechnology*, 23 (2012) 485203**.**
22 Yong K T, Sahoo Y, Zeng H, Swihart M T, Minter J R & Prasad P N, *Chem Mater*, 19 (2007) 4108.
23 Lee S H, Kim Y J & Park J, *Chem Mater,* 19 (2007) 4670.
24 Rojas-Chaveza H, Gonzalez-Dominguezb J L, Roman-Dovalc R, Juarez-Garciad J M, Daneue N & Rurik F, *Mater Sci Semiconduct Process*, 86 (2018) 128.
25 DeGroot M W, Taylorb N J & Corrigan J F, *J Mater Chem*, 14 (2004) 654.
26 Kuskovskya I L, Gongb Y, Neumarkb G F & Tamargo M C, *Superlatt Microstruct*, 47 (2010) 87.
27 Zhang B, Guo F & Wang W, *J Nanomater*, (2012) 293041.
28 Dwivedi D K, Dubey D & Dubey M, *J Ovonic Res*, 5 (2009) 35.
29 Sriram S, Chandiramouli R, Balamurugan D & Thayumanvan A, *Eur Phys J Appl Phys*, 62 (2013) 30101.
30 Xu S, Wang C & Cui Y, *J Mol Struct*, 938 (2009) 133.
31 Yadav P S & Pandey D K, *Adv Sci Eng Med*, 12 (2020) 930.
32 Gaussian, Inc (2003) *GAUSSIAN 03*, Revision C.03 (Pittsburgh, PA: Gaussian).
33 Olego D J, Raccah P M & Faurie J P, *Phys Rev B*, 33 (1986) 3819.